Supplementary Methods

Material and methods

Mice

WT CD4 T cells

Splenocytes were aseptically harvested from C57BL/6J mice. After gentle crushing of spleens through a 70 µM mesh filter, CD4+ T cells were isolated by negative selection using an EasySep Mouse CD4+ T cell Isolation Kit (StemCell Technologies, Grenoble, France). The purity exceeded 90%.

Scurfy CD4 T cells

Lymph nodes were collected from 10-day-old X^{Sf}/Y.Rag1$^{-/+}$ mice, and $CD4^+$ T cells were separated using a Murine $CD4^+$ T cell Isolation Kit (Miltenyi Biotec, Paris, France). The purity exceeded 90%. *Scurfy* $CD4^+$ T cells are highly sensitive to cell sorting and culture - probably as a consequence of being in a chronically activated environment. We optimized *scurfy* $CD4^+$ T cell sorting from lymph nodes to limit contamination by granulocytes and monocytes and to obtain a level of purity above 95%. The viability of *scurfy* $CD4^+$ T cells was improved (staying above 80% for up to 12 days in culture) by selecting donor mice younger than 12 days (to limit baseline inflammation) and by using 300 IU/mL IL-2 (compared with 100 IU/ml for WT $CD4^+$ T cells).

Wild-type Treg $CD4^+CD25^+$

Splenocytes and lymph nodes were harvested from B6LY5.1 CD45.1 mice (at 8 to 12 weeks of age) and $CD4^+$ T cells were isolated using an EasySep Mouse CD4+ T cell Isolation Kit. The $CD25^+$ cells were stained with an anti-CD25 phycoerythrin (PE) antibody (clone PC61, BD Biosciences, Le Pont de Claix, France). The $CD4^+CD25^+$ cells were then sorted on an SH800 (Sony Biotechnology, Weybridge, UK) or an ARIA II (BD Biosciences) cell sorter with a 100 µm nozzle. For the Treg suppression assay, $CD4^+CD25^-$ cells were also sorted.

The lentiviral vectors

The cDNAs for a truncated codon-optimized human ΔLNGFR and a codon-optimized human FOXP3 were cloned into a pCCL backbone with different designs. We generated eight vectors in total: four vectors expressing FOXP3 and the four corresponding mock counterparts containing only the *ΔLNGFR* reporter. Codon-optimized human FOXP3 was as follow:

>hFoxp3co sequence

```
atgcccaaccccagacccggaaagcctagcgccccttctctggccctgggaccttctcctggcgcctcc
ccatcttggagagccgcccctaaagccagcgatctgctgggagctagaggccctggcggcacattccag
ggcagagatctgagaggcggagcccacgcctctagcagcagcctgaatcccatgccccctagccagctg
cagctgcctacactgcctctcgtgatggtggcccctagcggagctagactgggccctctgcctcatctg
caggccctgctgcaggacagaccccacttcatgcaccagctgagcaccgtggatgcccacgccagaaca
cctgtgctgcaggtgcacccccctggaaagccctgccatgatcagcctgacccctccaaccacagccacc
ggcgtgttcagcctgaaggccagacctggactgccccctggcatcaatgtggccagcctggaatgggtg
tcccgcgaacctgccctgctgtgcaccttccccaatcccagcgccccagaaaggacagcacactgtct
gccgtgccccagagcagctatcccctgctggctaacggcgtgtgcaagtggcctggctgcgagaaggtg
```

```
ttcgaggaacccgaggacttcctgaagcactgccaggccgaccatctgctggacgagaaaggcagagcc
cagtgtctgctgcagcgcgagatggtgcagagcctggaacagcagctggtgctggaaaaagaaaagctg
agcgccatgcaggcccacctggccggaaaaatggccctgacaaaggccagcagcgtggccagctctgac
aagggcagctgctgcattgtggccgctggctctcagggacctgtggtgcctgcttggagcggacctaga
gaggcccccgatagcctgtttgccgtgcggagacacctgtggggcagccacggcaactctaccttcccc
gagttcctgcacaacatggactacttcaagttccacaacatgaggccccccttcacctacgccaccctg
atcagatgggccattctggaagcccccgagaagcagcggaccctgaacgagatctaccactggtttacc
cggatgttcgccttcttccggaaccaccccgccacctggaagaacgccatccggcacaatctgagcctg
cacaagtgcttcgtgcgggtggaaagcgagaagggcgccgtgtggacagtggacgagctggaatttcgg
aagaagcggtcccagaggcccagccggtgtagcaatcctacccctggcccttga
```

- Two vectors had a bidirectional promoter architecture: one allowed FOXP3 expression under the control of the EF1α and *ΔLNGFR* expression under the control of the PGK promoter (LNGFRp-eFOXP3 and LNGFRp-e, respectively), and the other allowed *FOXP3* expression under the control of PKG and ΔLNGFR under the control of EFS (LNGFRe-pFOXP3 and LNGFRe-p, respectively). A unidirectional polyA sequence was added to terminate transduction of the reverse gene.
- Two bicistronic vectors were created (using the 2A self-cleaving peptide system) to allow the co-expression of FOXP3 and *ΔLNGFR* (namely eLNGFR.t2a.FOXP3 and eLNGFR.t2a versus. eFOXP3.t2a.LNGFR and e.t2a.LNGFR) (Fig. 1A).

Lentiviral vectors were packaged with a vesicular stomatitis virus G pseudo-type, as described previously. Production of bidirectional constructs was stimulated by co-transfection with the NovB2 plasmid (1).

Determination of the vector copy number

Genomic DNA was extracted from samples 12 days after transduction, using a Genomic DNA Purification kit (Qiagen, Cergy-Pontoise, France). The VCNs were quantified using a quantitative real-time polymerase chain reaction (qPCR) or a droplet digital PCR (ddPCR). The qPCRs were performed according to a protocol described previously [16]. For ddPCR, gDNA was first digested with Hind III HF (New England Biolabs, Evry, France), and mixed with ddPCR Mastermix (Bio-Rad, Marnes-la-Coquette, France) and primers and probes specific for the HIV Psi region (Bio-Rad) and a sequence in the murine genome (Titin). Droplet generation was performed using the QX100 Droplet system. The concentration of specific amplified portions was quantified using the QX200 Droplet Reader/Quantasoft V1.7 (Bio-Rad).

***In vitro* titration assay**

HCT116 cells were kindly provided by Olivier Danos (Genethon, Evry, France). Cells were maintained in DMEM medium + Glutamax (GIBCO) with 1% penicillin-streptomycin (GIBCO) and then transduced with escalating doses of the different vectors. The respective titers were evaluated using qPCRs.

Flow cytometry

Single-cell suspensions from the spleen and lymph nodes were obtained by gentle crushing of spleens through a 70 µM mesh filter. Samples from the lung and the liver were prepared after digestion with Collagenase IV (Thermo Fisher Scientific), followed by gentle crushing of spleens through a 100 µM mesh filter.

Samples were prepared for flow cytometry as follows: cells were re-suspended in 100 uL of FACS buffer (PBS [Corning] with 2% fetal bovine serum [GIBCO]) and incubated with 2 uL of each antibody and 7AAD (Miltenyi Biotec) for 20-30 min at 4 C.

Cells were washed once in FACS buffer prior to analysis. For intracellular FOXP3 staining, cells were first stained with cell surface markers and fixable viability dye eF780 (eBioscience, Thermo Fisher Scientific), as described above. After washing, cells were fixed and permeabilized using the FoxP3 staining buffer set (eBioscience, Thermo Fisher Scientific), according to the manufacturer's instructions. Human FoxP3-APC (eBioscience, Thermo Fisher Scientific) was added for 30-60 min at room temperature. Samples were acquired on a MACSquant flow cytometer (Miltenyi Biotec), a BD LSR Fortessa cytometer (BD Biosciences) or a Sony Spectral SH6800 cytometer (Sony Biotechnology). Data were analyzed using FlowJo software (version 10, TreeStar, BD Biosciences). The following antibodies were used: anti-mouse CD62L APC-Cy7 clone MEL-14, CD44 APC clone IM7 (BD Biotechnology), CD45.1 APC-Cy7 clone A20, CD45.2 PeCy7 clone 104, CD25 clone PC61 Brilliant Violet 711, CD152 clone UC10-4B9 PE/Dazzle (Sony Biotechnology), human ΔLNGFR PE clone ME20.4-1.H4 (Miltenyi Biotec), Helios clone 22F6 eF450, and human FOXP3 APC Clone PCH101 (eBioscience, Thermo Fisher Scientific).

Transcriptomic analysis

On day 50 (35 days after adoptive transfer), 1000 CD45.1 or $LNGFR^+$ $CD4^+$ T cells were sorted twice from lymph nodes (using a flow cytometer (SH800, Sony Biotechnology, Weybridge, UK)) directly into 5 µl lysis buffer. Smart-seq2 libraries for ultra-low-input RNA-seq were prepared as described previously [17,18], with some slight modifications (see the Supplementary Methods). Samples were sequenced on an Illumina NextSeq500 system, using the 2 x 25 bp read option with no further trimming. Transcripts were quantified using the Broad Technology Labs computational pipeline (2). Normalized reads were further filtered and analyzed using Multiplot Studio in the GenePattern software package (https://www.genepattern.org/modules/docs/Multiplot/2) and R Studio® (version 1.2.5019, RStudio Team 2020, PBC, Boston, MA, United States, http://www.rstudio.com/). To reduce noise, only genes with a coefficient of variation between biological replicates <0.3 in either comparison group, and with at least one sample with an expression value >30 were selected. A total of 10086 transcripts were analyzed.

Statistical analysis

Data were quoted as the mean ± SD, unless stated otherwise. All statistical analyses were performed with GraphPad Prism software (version 8.0, GraphPad Software, Inc., San Diego, CA). Statistical tests included the non-parametric Mann-Whitney test, Fisher's exact test, and a two-way ANOVA, depending on the dataset. The threshold for statistical significance was set to $p<0.05$. In figures, statistically significant intergroup differences were noted with asterisks (*$p < 0.05$, **$p < 0.01$, ***$p < 0.001$, ****$p < 0.0001$). Correlations were assessed by calculation of Spearman's non-parametric correlation coefficient. Survival was analyzed with a log-rank (Mantel-Cox) test. Differential gene expression was analyzed using Multiplot software (Regents of the University of California, Broad Institute, MIT). Enrichment in the Treg signature was assessed with a chi-squared test.

Transcriptomic analysis

After the final sorting of 1000 cells directly into 5 µl of lysis buffer, Smart-seq2 libraries were prepared as previously described (2, 3), with slight modifications. Briefly, total RNA was captured and purified on RNAClean XP beads (Beckman Coulter). Polyadenylated mRNA was then selected using an anchored oligo(dT) primer (5′–AAGCAGTGGTATCAACGCAGAGTACT30VN-3′) and converted to cDNA by reverse transcription. First-strand cDNA underwent limited PCR amplification and then Tn5-transposon-based fragmentation using the Nextera XT DNA Library Preparation Kit (Illumina). Samples were then PCR-amplified for 18 cycles using barcoded primers, such that each sample carried a specific combination of eight base Illumina P5 and P7 barcodes. The samples were pooled before smart-seq paired-end sequencing on an Illumina NextSeq500 system using 2 x 25 bp reads and no further trimming. Reads were aligned with the mouse genome (3) using STAR software (version 2.5.4a) (4). The ribosomal RNA gene annotations were removed from the General Transfer Format file. The gene-level quantification was calculated using feature Counts (5). Raw read count tables were normalized using the median of ratios method with the DESeq2 package from Bioconductor (6) and then converted to GCT and CLS format. Samples with less than 1 million uniquely mapped reads were automatically excluded from normalization, in order to mitigate the effect of poor-quality samples on the normalized counts. Processed samples having fewer than 8,000 genes with over ten reads were removed from the dataset, to eliminate the effect of samples with potential PCR amplification errors. All samples were also screened for contamination by using known cell-type-specific transcripts (according to ImmGen database www. http://www.immgen.org/). Using Pearson's correlation test, we screened biological replicates for poor-quality samples and then removed them from the dataset. To avoid outlier effects, Pearson's correlation coefficient was calculated for transcripts with an average of more than five reads or ranked below the 99th percentile for the number of reads in the dataset. Any replicates that did not have a Pearson's coefficient of 0.9 or more were removed from the dataset prior to downstream analysis. Lastly, the RNA integrity in all samples was measured by median transcript integrity number for mouse housekeeping genes (5), using RSeQC software (7). Samples with a transcript integrity number < 45

were removed from the dataset before downstream analysis.

Supplemental Table 1. The *scurfy* disease scores

To enable the reproducible evaluation of the *scurfy* mice phenotype, we developed a specific score for the signs of *scurfy* disease (blepharitis, ear eczema, whole-body eczema, tail eczema, limb edema, body weight, the mouse's appearance, and the mouse's behavior) on a scale from 0 to 21. Each item in the *scurfy* score was weighted according to the lesion's description or extension. The score was validated in a group of more than 50 mice by two independent experimenters.

Supplemental Table 2. The Treg signature score

To provide a quantitative estimate of the Treg signature establishment, we computed a "signature score" for each gene in the Treg upregulated signature, where 0 and 1 correspond to expression in Tconv (CD4.LNGFR) and Treg cells, respectively.

Supplemental Figure 1. Therapeutic strategies for late Treg adoptive transfer

A-C. *Scurfy* males (X^{Sf}/Y.Rag1$^{+/-}$ on a CD45.2 background) were treated with a subcutaneous injection of 2 mg/kg temsirolimus on day 8 and day 10 and received 5x10^5 congenic CD45.1 WT Treg on day 14. Next, 2 mg/kg temsirolimus was injected subcutaneously twice a week. All mice were sacrificed on day 28 for flow cytometry analysis. B. *Scurfy* scores were recorded daily, and no significant differences were observed with Treg treatment. C. To monitor Treg engraftment, CD45.1 chimerism (gated on CD4$^+$ T cells) was analyzed in the lymph nodes and spleen.

D-F. *Scurfy* males (X^{Sf}/Y.Rag1$^{+/-}$ on a CD45.2 background) were treated with a daily subcutaneous injection of anti-CD3 Fab'2 (AntiCD3, 20 µg/day) for 5 days from day 8 of life and received 5x10^5 congenic CD45.1 WT Treg on day 14. E. *Scurfy* scores were recorded until day 35; no significant differences between Treg treatment groups were observed. F. CD45.1 chimerism (gated on CD4$^+$ T cells) was analyzed in the lymph nodes and spleen on day 35.

G-I. *Scurfy* males (X^{Sf}/Y.Rag1$^{+/-}$ on a CD45.2 background) were treated with a 150 mg/kg i.p. injection of cyclophosphamide (Cy) on day 10 of life and received 5x10^5 congenic CD45.1 WT Treg on day 14. H. *Scurfy* scores were recorded; no significant differences between Treg treatment groups were observed. I. CD45.1 chimerism (gated on CD4$^+$ T cells) was analyzed in the lymph nodes and spleen. On day 76 of life, transferred C45.1 Treg were barely detectable.

Supplemental Figure 2. Determination of the inhibition of *scurfy* symptoms according to the dose of injected $CD4^{LNGFR.FOXP3}$ cells

A-D. *Scurfy* males (X^{Sf}/Y.$Rag1^{+/-}$ on a CD45.2 background) were conditioned by an IP injection of 50 mg/kg cyclophosphamide on day 10 of life and received $5x10^5$ congenic CD45.1 WT Treg or $CD4^{LNGFR.FOXP3}$ transduced cells at three different doses ($0.5x10^6$; $0.75x10^6$ or $1x10^6$ cells) on day 14. Next, 1000 IU/g IL-2 was injected i.p. once a day for 5 days and then once a week (n≥3 per group).

B. CD45.1 chimerism (gated on $CD4^+$ T cells) was analyzed in the lymph nodes, spleen, blood, lung, and liver in mice treated with Treg on day 50.

C. ΔLNGFR chimerism (gated on $CD4^+$ T cells) was analyzed in the lymph nodes, spleen, blood, lung and liver in mice treated with $CD4^{LNGFR.FOXP3}$. The mean ± SD value is shown.

D. Representative flow cytometry analysis of CD62L staining, gated on $CD4^+$ T cells. Treatment with Treg or $CD4^{LNGFR.FOXP3}$ cells restored a subset of CD62L-positive $CD4^+$ T cells.

Supplemental Figure 3. Engineered *scurfy* CD4 T cells with LNGFR.FOXP3 vector rescue *scurfy* mice after disease onset

A. Representative pictures of *scurfy* mice on day 50. Mice treated with vehicle (Cy+IL-2+PBS) and with $CD4^{LNGFR}$ cells did not recover from Cy-induced alopecia. Skin, ear and tail lesions are also shown. In contrast, mice treated either with Treg or $CD4^{LNGFR.FOXP3}$ cells recovered from Cy-induced alopecia, displayed only limited tail and eye eczema, and showed a recovery in growth.

B. Representative dot plots of FOXP3 and ΔLNGFR expression levels (measured by flow cytometry) for $CD4^+$ T cells collected from the lymph nodes on day 50 in mice receiving $CD4^{LNGFR.FOXP3}$ cells, $CD4^{LNGFR}$ cells or PBS.

C. On day 50, $\Delta LNGFR^+$ cells were selected from lymph node $CD4^+$ T cells for quantification of the VCN in mice treated with $CD4^{LNGFR.FOXP3}$ cells or $CD4^{LNGFR}$ cells.

D. Representative CD62L staining experiments demonstrated that a subset of $CD62L^+$ cells was restored in $CD4^+$ T cells from the lymph nodes in mice treated with Treg and $CD4^{LNGFR.FOXP3}$ cells (percentage of $CD62L^+$, gated on $CD4^+$ T cells).

E. Representative dot plots illustrating CD45.1 and CD45.2 chimerism (measured by flow cytometry) in $CD4^+$ T cells from the lymph nodes collected on day 100 from mice treated with Treg (upper panel).

FOXP3 and ΔLNGFR expression levels were measured (using flow cytometry) on $CD4^+$ T cells from lymph nodes collected at day 100 from mice treated with $CD4^{LNGFR.FOXP3}$ cells (lower panel).

Supplemental Figure 4. $CD4^{LNGFR.FOXP3}$ cells partly maintain the Treg signature after adoptive transfer on day 50 of life

A. Normalized expression levels of human *Foxp3 (*from heathy donor Tregs or codon optimized sequence in human healthy donor Tregs (green star), $CD4^{LNGFR}$ cells (purple dot), $CD4^{LNGFR.FOXP3}$ cells (blue dot) and WT Treg (salmon dot) sorted from the corresponding treated mice. Each dot represents cells sorted from the same mouse. The Y-axis is a log10 scale.

B. Normalized expression levels of mouse *Foxp3 (*WT or *scurfy* mutant) in $CD4^{LNGFR}$ cells (purple dot), $CD4^{LNGFR.FOXP3}$ cells (blue dot) and WT Treg (salmon dot) sorted from the corresponding treated mice. Each dot represents cells sorted from the same mouse. The Y-axis is a log10 scale.

C. A volcano plot (the FC versus the *P* value) of the transcriptomes of $CD4^{LNGFR.FOXP3}$ cells versus WT Treg on day 50. The Treg upregulated signature (in red), downregulated signature (in blue) and core Treg gene annotations are highlighted. The values in the upper half represent the number of corresponding Treg signature genes induced (right) or repressed (left), with the number of upregulated signature genes in red and the number of downregulated signature genes in blue.

References

1. T. Maetzig, M. Galla, M. H. Brugman, R. Loew, C. Baum, A. Schambach, Mechanisms controlling titer and expression of bidirectional lentiviral and gammaretroviral vectors, *Gene Ther.* **17**, 400–411 (2010).
2. C. Trapnell, A. Roberts, L. Goff, G. Pertea, D. Kim, D. R. Kelley, H. Pimentel, S. L. Salzberg, J. L. Rinn, L. Pachter, Differential gene and transcript expression analysis of RNA-seq experiments with TopHat and Cufflinks, *Nat. Protoc.* **7**, 562–578 (2012).
3. S. Picelli, Å. K. Björklund, O. R. Faridani, S. Sagasser, G. Winberg, R. Sandberg, Smart-seq2 for sensitive full-length transcriptome profiling in single cells, *Nat. Methods* **10**, 1096–1100 (2013).
4. S. Picelli, O. R. Faridani, Å. K. Björklund, G. Winberg, S. Sagasser, R. Sandberg, Full-length RNA-seq from single cells using Smart-seq2, *Nat. Protoc.* **9**, 171–181 (2014).
5. https://www.gencodegenes.org/mouse_releases/16.html.
6. Releases · alexdobin/STAR · GitHub (available at https://github.com/alexdobin/STAR/releases).
7. The Subread package (available at http://subread.sourceforge.net/).

Supplemental figure 1

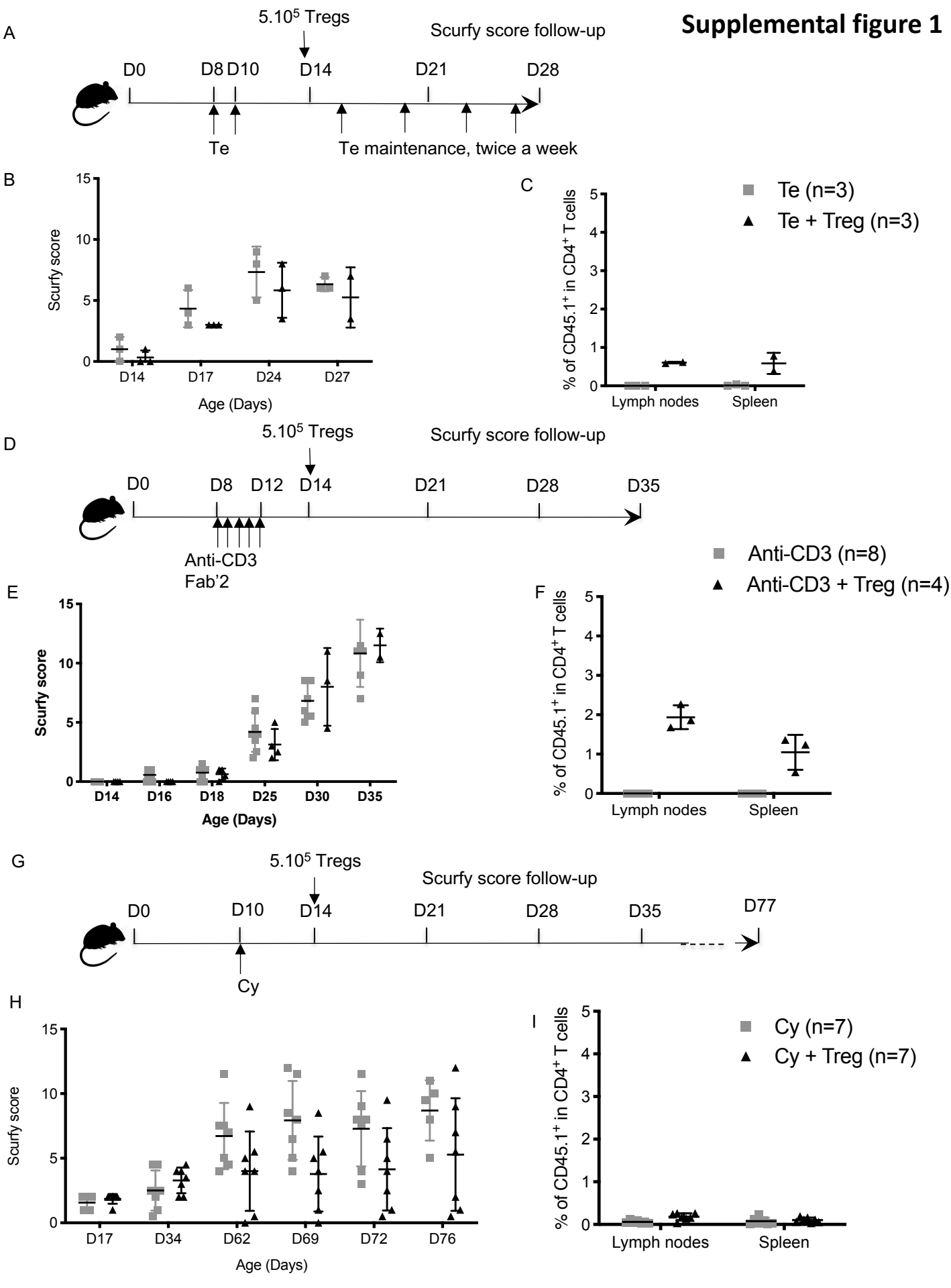

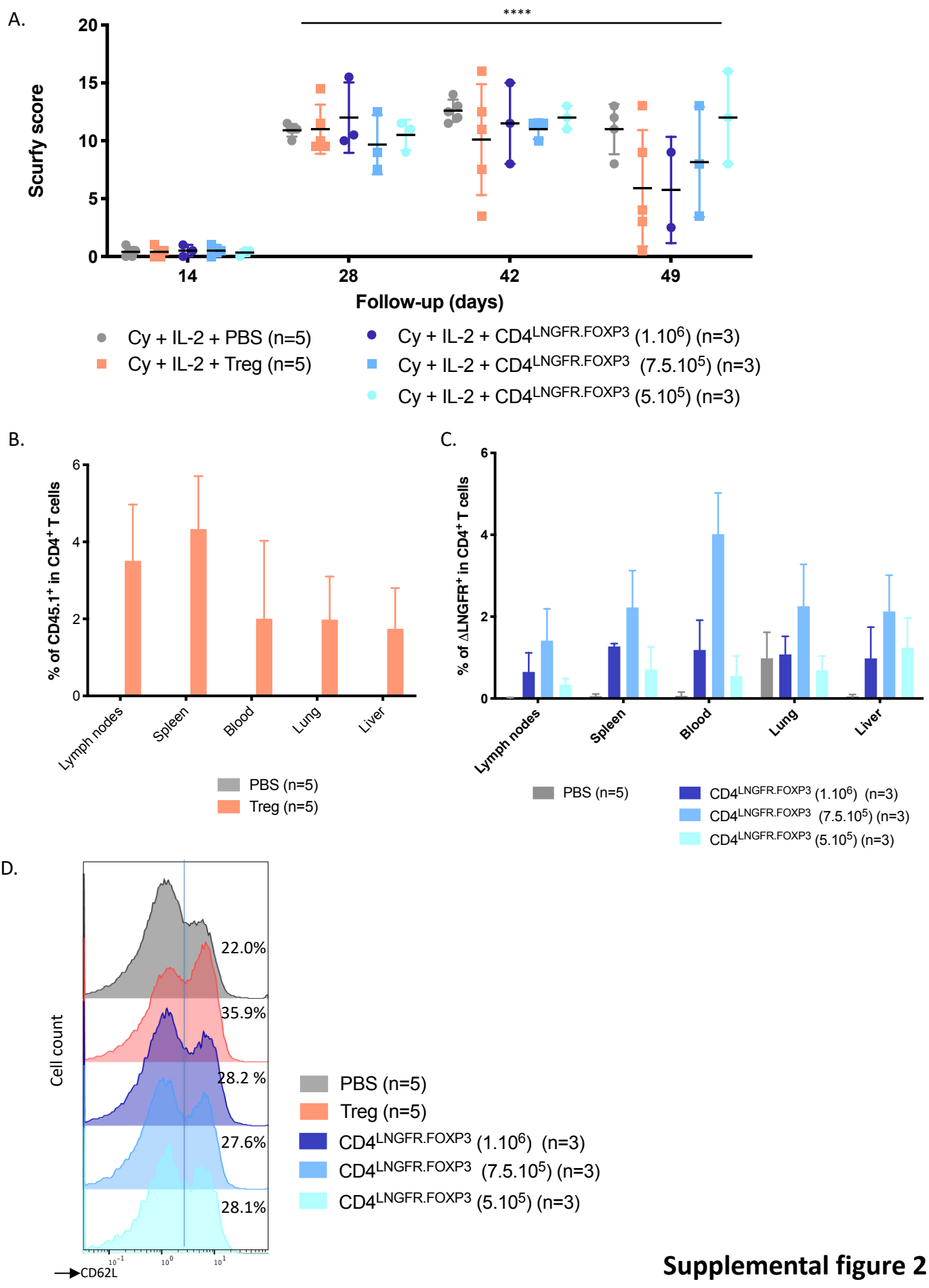

Supplemental figure 2

Supplemental figure 3

A.

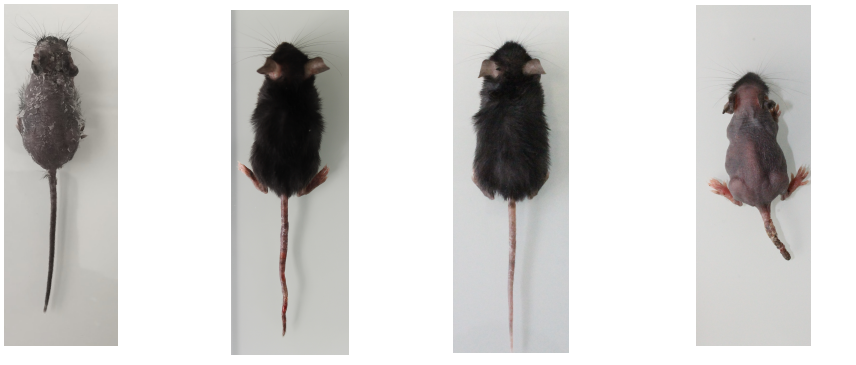

B.

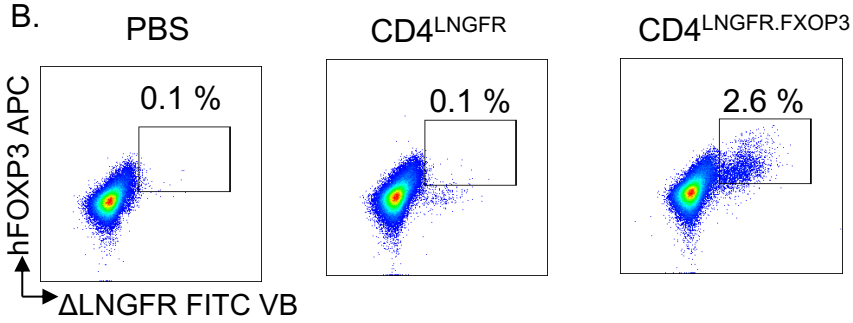

C.

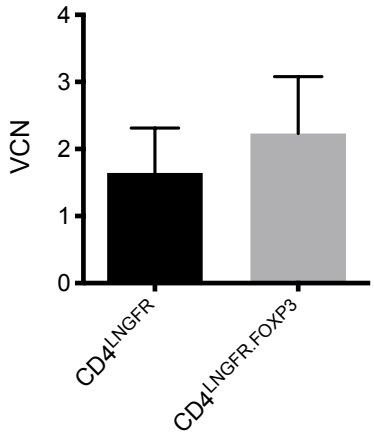

D.

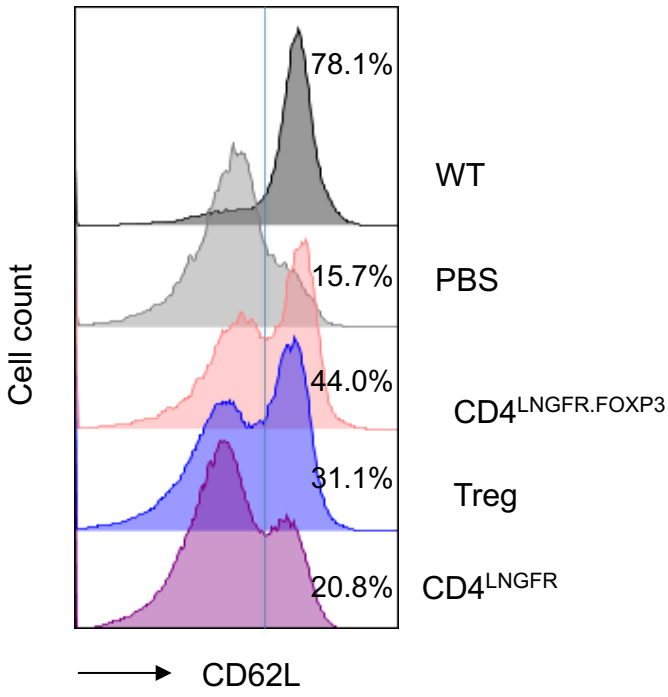

E.

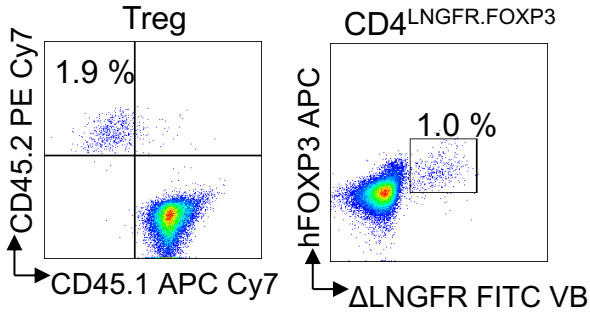

Supplemental figure 4

A

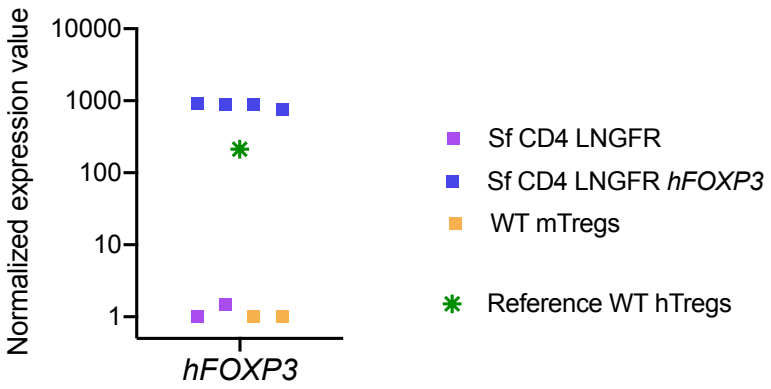

B

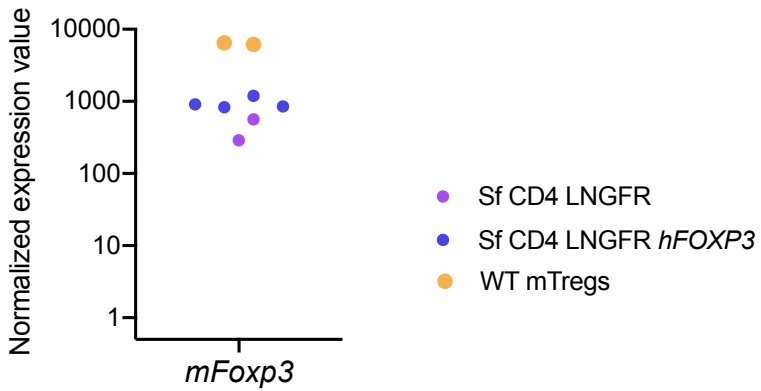

C